SCANNING ELECTRON MICROSCOPY OF FRACTURE SURFACES OF CARBON COMPOSITE MATERIALS

W.G.J. 't Hart

March 1976

19960321 032

DISCLAIMER NOTICE

UNCLASSIFIED

Technical Report
distributed by

**DEFENSE
TECHNICAL
INFORMATION
CENTER**

DTIC Acquiring Information-
Imparting Knowledge

Cameron Station
Alexandria, Virginia 22304-6145

UNCLASSIFIED
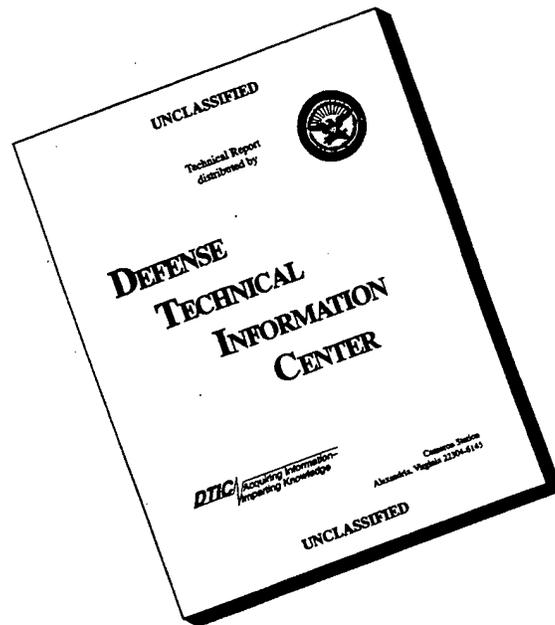
THIS DOCUMENT IS BEST QUALITY AVAILABLE. THE COPY FURNISHED TO DTIC CONTAINED A SIGNIFICANT NUMBER OF PAGES WHICH DO NOT REPRODUCE LEGIBLY.

NATIONAAL LUCHT- EN RUIMTEVAARTLABORATORIUM

NATIONAL AEROSPACE LABORATORY NLR

THE NETHERLANDS

NLR TR 76035 U

SCANNING ELECTRON MICROSCOPY OF FRACTURE SURFACES

OF CARBON COMPOSITE MATERIALS

BY

W.G.J. 't HART

NLR

	ORIGINATOR'S REF. NLR TR 76035 U		SECURITY CLASS. Unclassified

ORIGINATOR National Aerospace Laboratory NLR
Amsterdam. The Netherlands

TITLE

Scanning electron microscopy of fracture surfaces of

carbon composite materials

PRESENTED AT

AUTHORS W.G.J. 't Hart	**DATE** March 1976	**pp** 29	**ref** 18

DESCRIPTORS

Carbon fiber reinforced plastics   Failure modes
Fatigue (materials)   Carbon fibers
Fractures (materials)   Shear strength
Fracture strength
Fractography
Electron microscopes   DATE OF PUBLICATION
Metal surfaces   JAN 1979

ABSTRACT

A microscopic study has been performed on carbon composite
fracture surfaces, using the Scanning Electron Microscope (SEM). It
appears that the SEM is a useful tool to examine the fracture surface
characteristics of composite materials failing under different loading
conditions.

NLR TR 76035 U

SCANNING ELECTRON MICROSCOPY OF FRACTURE SURFACES OF CARBON COMPOSITE MATERIALS
by

W.G.J. 't Hart

SUMMARY

A microscopic study has been performed on carbon composite fracture surfaces, using the Scanning Electron Microscope (SEM). It appears that the SEM is a useful tool to examine the fracture surface characteristics of composite materials failing under different loading conditions.

Division:	Structures and Materials	Completed	: March 1976
Prepared:	WGJ'tH	NIVR contractnumber	: 1744
Approved:	HPvL	Ordernumber	: 101.323
		Typ.	: MW

CONTENTS

1   INTRODUCTION

The potential of advanced composite materials has been demonstrated in numerous studies in recent years. Many structural components have already been constructed and are in service for several years, reference 1,2. However, most of the structural applications of composites up to now are based on stiffness, rather than strength criteria. The composite reinforcement is usually adapted to the expected loading direction, but the most efficient use for filamentary composites is for unidirectional load transmission.

Elastic properties as well as the fracture behaviour of unidirectional (u.d.) composites depend on the properties of the constituent components. The stiffness of a composite can be determined very well by using the "rule of mixtures" (R.O.M.). The strength properties are more influenced by the variation in strength of the reinforcing fibres. Fracture under tensile, compressive, shear, and fatigue loading has been studied by many authors and has resulted in numerous failure criteria (Ref. 3 to 8).

The different fracture processes are accompanied by characteristic fracture surfaces. A proper interpretation of the characteristic fracture markings provides valuable information concerning the mechanism of failure and enables evaluation of theoretical studies on fracture- and fatigue processes.

In the present investigation a macroscopic and microscopic study has been performed on composite fracture surfaces in order to relate the fracture surface characteristics to the fracture mechanisms and the type of loading.

To facilitate interpretation of the photographs there is first a theoretical explanation concerning the possible fracture processes expected to occur under different loading conditions.

2   FRACTURE PHENOMENA IN COMPOSITES

A u.d. composite material consists of strong and stiff fibres embedded in a comparatively weak matrix. The fibres sustain the load. Advanced fibres such as boron and carbon fibres have a tensile

strength > 2500 MN/m^2 and a stiffness > 240 $\frac{GN}{m^2}$, but they are extreme-
ly brittle. No plastic deformation occurs at fracture load. The fibre
strength can be characterized by a statistical strength distribution
function. For advanced fibres the coefficient of variation of the mean
strength will usually be 0.1 < c.v. < 0.2.

Although the strength properties of the matrix are low in comparis-
on with the fibre properties, the important role of the matrix is
evident from the following functions:

- The matrix binds the fibres together, holds them aligned in the
  stressed direction, and permits the composite to be loaded.
- The matrix protects the fibres from mechanical damage and it
  determines the corrosion resistance of the composite.
- If the matrix is ductile (metal matrix composites) it provides a
  mechanism for slowing down the propagation of cracks that may
  initiate at broken fibres.
- The matrix is able to redistribute the load of broken fibres by
  shear stresses among the adjacent fibres.

Besides proper fibre and matrix properties, the fracture behaviour
of a composite under loading is controlled by the interface between
fibre and matrix. The interface consists of the bond between fibre
and matrix and the immediate region adjacent to this bond. The type
of bonding can be of chemical or mechanical nature.

The role of the fibre/matrix bond is important since the struct-
ural efficiency of a composite material depends on the ability of the
interface to transfer shear load from the matrix to the fibres. A
better understanding of the important role of the interface is obtain-
ed when it is realized that 1 cm^3 of a u.d. composite (V_f=50%) with
fibres of $\emptyset$ 8 µm diameter contains approximately 2500 cm^2 of inter-
face area.

Before the influence of the interface bond on the fracture
mechanism is reviewed, the nature of the interface will be discussed
first.

2.1   The fibre/matrix interface (Ref. 10)

        The quality of the fibre/matrix bond depends on:

    i.   the wettability of the fibre surface

    ii. the chemical reactivity between fibre and matrix

i. Poor wetting will produce voids at the interface leading to crack
initiation due to stress concentrations. In order to obtain complete
wetting of a surface, the matrix must be initially of low viscosity.
Furthermore, the wettability depends on the surface tensions of matrix
and fibre and the interface, which will be considered below.
The surface tension of a liquid or solid with respect to a vapour
phase, tends to decrease the surface area between the two phases.
When a droplet of a liquid is in contact with a solid, the three forces
which try to contract the three surfaces are in equilibrium.

$$\gamma_{SV} = \gamma_{SL} + \gamma_{LV} \cos \theta \tag{1}$$

where S, V and L stand for solid, vapor and liquid, (Fig. 1).

    Small values of θ result in a good wettability. The contact angle
θ not only varies with temperature, but also is extremely sensitive
to the adsorption of impurities on the surface of the solid, i.e. the
fibre surface, table 1.
Usually the contact angle for combinations of liquid resins with
carbon, boron and glass fibres is so small as to indicate a good wetting.
However, when boron and carbon fibres are embedded in a metal matrix
such as aluminium, wetting problems will arise. Figure 2 shows the
contact angle of aluminium on carbon as a function of temperature.
Coupling agents can be applied to improve the surface wettability. The
application of a titanium coating (TiC) on carbon fibres produces a
sharp decrease in θ (improved wettability). Boron fibres for metal
matrix composites are usually coated with silicon carbride (SiC) to
improve the wettability as well as to protect the fibre against fibre
degradation by the liquid metal during the fabrication process.

ii. Chemical reactivity depends upon the ability of functional groups on
the fibre surface to react with the matrix. Glass fibre coatings, for
example, contain chemical functional groups which can react with
silanol groups on the glass surface, and other functional groups which
can co-react with the resin during cure. The interface strength of
carbon/epoxy is dependent on the surface condition of the fibre. The

surface of the fibre is rather smooth. In the early development of carbon/epoxy composites, the interlaminar shear strength was below expectation due to the inability of such fibres to adhere tenaciously to the resin. In the United States this has resulted in turning to other reinforcements such as boron. However, the British research laboratories developed a surface treatment which led to considerable improvement of the interface strength between fibre and resin. Today most of the carbon/epoxy composites have been made of surface treated carbon fibres. The surface treatment may involve a cleaning process, or an oxidation process in concentrated nitric acid, to create functional groups which can react with the resin matrix. Boron fibres are not surface treated since the corn-cob surface structure provides sufficient irregularity for a good interface bond.

2.2 Interface and mode of failure

The influence of the interface bond on the fracture mechanisms of composites for different loading conditions will be explained in the following theoretical considerations.

- composite under tensile loading (Fig. 3 and 4).

When loading a u.d. composite the weakest fibres will break first. Load concentrations will be created in the adjacent fibres and the strength of the interface bond determines the magnitude of these load concentrations. If the interface bond is very strong, no debonding occurs and the load is transferred to the adjacent fibres over a short distance and results in high load concentrations. These load concentrations may cause cracking of the matrix resulting in a propagating crack through the next fibre. This type of interface bonding results in a brittle fracture and the fracture surface will be fairly smooth without fibre pull-out.

An intermediate bond strength may result in partial debonding, and a propagating crack which is blunted by crack propagation parallel to the fibres. The fracture surface will be somewhat irregular, with features of fibre pull-out. If there is a distinctly weak interfacial bond the fracture surface exhibits marks of pronounced irregularity and fibre pull-out.

A strong interface bond will contribute to the "weakest link" failure mode resulting in a low ultimate composite strength. A high ultimate

tensile strength can be expected for a composite material with an intermediate bond strength, reference 18.

- composite under compressive loading

The following initial failure modes can be expected when a u.d. composite is loaded in compression

- fibre microbuckling, the matrix still elastic (low V_f).
- matrix yielding followed by fibre microbuckling (metal matrix composites).
- interface debonding followed by fibre microbuckling.

Macroscopically, the initial failure modes may involve a shear failure. No fibre pull-out can be expected and the fracture surface will be rather smooth.

- composite under 3 point bend loading

The quality of the fibre/matrix bond is usually measured by a three point bend test. Depending upon the span-to-depth ratio either shear failure or a flexural failure will occur (Fig. 5). If a sufficiently small ratio is chosen, a shear mode of failure is favoured in the neutral plane, resulting in a maximum value for the interlaminar shear stress (ILSS). Larger span-to-depth ratios result in a complex flexural failure, and the calculated ILSS decreases.

The fracture surface of a flexural failure will be characterized by two distinctly different surfaces connecting with the tensile and compressive stresses. The quality of the fibre/matrix bond can be deduced from the amount of fibre pull-out on the tensile side of the specimen.

- composite under fatigue loading

Fatigue testing of u.d. composites under axial fatigue loading may result in a fatigue strength of 70% of the ultimate load at 10^7 cycles for $R > 0$ (Ref. 8). Fatigue has been found to be much more significant under conditions of shear loading, both interlaminar and torsional. The fatigue failure of cross plied laminates under axial constant amplitude loading is initiated mostly at specimen edges, owing to shear forces between the constituent layers. The fatigue life of cross plied laminates is determined by the interlaminar shear strength rather than the interface bond strength. Delamination will be accompanied by a relatively flat fracture surface.

3   THE SCANNING ELECTRON MICROSCOPE AND COMPOSITE FRACTURE SURFACES
     (Ref. 11, 12, 13)

In the present investigation a Scanning Electron Microscope
(SEM) type Cambridge Stereoscan S4-10 was used to study the character-
istic marks on composite fracture surfaces. The irregular topography
of the fracture surfaces does not allow accurate observations by
conventional techniques of optical or transmission electron micros-
copy (TEM).

To investigate a fracture surface a primary condition is that
the specimen is electrically conducting. Carbon fibres are conducting
but not the surrounding epoxy matrix. In order to make the surface
entirely conducting a gold coating was vacuum deposited on the specimens.
A maximum acceleration voltage of 10 kV was used in order to prevent
surface damage by the electron beam.

4   COMPOSITE FRACTURE SURFACES

The types of investigated specimens and their mechanical propert-
ies are given in table 2. The fibre volume fraction was 45 to 65% and
the matrix systems were unmodified epoxy resins. The composite material
was fully cured according to the specifications of the manufacturer.

In this section low magnification and SEM photographs of fracture
surfaces will be discussed for the different modes of failure.

- Tensile fracture
Low magnification photographs of a tensile fracture are shown in
figure 6. The specimen was "waisted" in the thickness direction in
order to prevent failure in the grips. Failure occurred in the thinnest
section. In one part of the specimen delamination occurred, indicating
that the waisting procedure introduced stress concentrations leading
to shear stresses exceeding the interlaminar shear strength. Figure 6
shows a rather straight fracture surface, indicating a good interface
strength (although a straight fracture surface is also partly caused
by the waisting procedure).
Figure 7 presents an SEM photograph of the fracture. There is only

slight fibre pull-out. Clusters of fibres have been broken with
resin adhering to the fibres. This indicates that there is a strong
interface since clusters of fibres then react as integral units and
fracture will initiate from weak planes rahter than from each
individual fibre.

- Compressive fracture

The macroscopic appearance of a compressive fracture of a carbon/
epoxy specimen is a relatively smooth fracture surface at an angle of
45 to 60° with the loading direction (Fig. 8 and 9). During the
fracture process interlaminar cracks can be formed and local buckling
can occur, resulting in an irregular, stepped fracture surface (Fig. 9).

Usually the compressive strength of carbon/epoxy will be lower
than the tensile strength. This is probably due to the small diameter
of the fibres, which can be supported less effectively by the matrix
than larger diameter fibres, e.g. boron.

At high magnification it can be observed that fibre parts have
been spread over the surface (Fig. 10). Accurate examination of single
fibres shows that some failed by microbuckling. The buckling occurred
for a number of fibres in the same direction, thereby indicating a
general buckling failure for parts of fibres integral with the matrix.
The occurrence of buckling will depend on the interface strength.
Examination of a large area on the fracture surface was not possible,
owing to damage of the fracture surface by the failure process.

- Flexural fracture

The ILSS and flexural strength were investigated by a three point
bend test of a short beam specimen. It was anticipated that the fract-
ure process might be a combination of shear- and flexural fracture.
The load-displacement curves associated with the different fracture
modes are shown in figure 11.

Considering the fracture surface of the investigated specimen
at a low magnification, smooth and rough areas are observed (Fig. 12).
The smooth area is the result of a compressive failure. The fibrous
appearance of the other part indicates fibre pull-out under tensile
stresses.

From the low magnification photographs it can be concluded that
fracture was the result of flexure rather than shear. However, an SEM

photograph taken form the transition zone also shows interlaminar shear cracks, developed at the neutral plane, figure 13. Away from the neutral plane less shear cracks are observed, figure 14, 15. The flexural failure mode has therefore probably been initiated by shear forces.

The tensile part of this beam specimen shows a considerable fibre pull-out, figure 13. No resin parts adhere to the broken fibres and clusters of fibres have not broken as intergral units. Thus, the interface bond was not so good as the interface bond in the tensile specimen discussed previously (compare Fig. 7 and Fig. 13).

Examination of the fracture surfaces of single fibres shows that fibres failed due to tensile loading and by microbuckling under compressive loading.

Figure 14 to 16 show a large number of fibres failed by microbuckling. The actual loading direction can be derived from the buckling orientation, since buckling of all the fibres occurred in the same direction.

From figure 16 it can be seen that surface wetting of the fibres by the resin was very good. At the bottom of some fibres in figure 16, several matrix cracks have initiated in a radial direction. These cracks probably originated at the circumference of fibres under influence of a combination of residual shrinkage stresses in the matrix and additional stresses due to the fracture process. A theoretical consideration of Chamis (Ref. 9) on residual stresses in polymer matrix composites shows that the resin hoop stress might reach 40 MNm^{-2}, figure 17. The order of magnitude of the tensile strengths of epoxy resins is 50 to 100 MNm^{-2}. The crack orientation is such that no influence on tensile fracture can be expected.

Purely tensile fracture surfaces of single fibres are shown in figures 18 and 19. The fracture surface appearance can be related to the theoretical model of the carbon fibre, reference 14, 15. The precursor of most carbon fibres is polyacrilonitrile. The liquid polymer is pressed through a spinneret having 10,000 microscopic holes, and a silvery white string is obtained. In a stretched condition the strings undergo oxidation and carbonization stages. The initial stretching and the shrinkage during processing helps to increase the axial alignment of the polymer molecules. During processing a ladder struct-

ure is formed, and after eliminating the remaining hydrogen and nitrogen, the carbon atoms form ribbons of a hexagonal network, figure 20. The network ribbons are strong and stiff in the two basic directions of the basal plane, but weak in the direction perpendicular to the basal plane.

A carbon fibre with a diameter of about 8 μm consists of some 100 or more ribbons (fibrils) with a certain degree of ordening to the fibre axis, figure 21. The fibre surface is smooth but the fibrils are visible at high magnifications, e.g. figure 18.

Figure 19 shows a peculiar shape for a carbon fibre, namely a hollow fibre. It is not clear whether this exceptional shape is due to the spinning process or is caused by "internal oxidation" of the PAN fibre.

If a carbon fibre is not loaded by a uniform tensile stress, crack initiation may occur at the circumference of the fibre. This is what happened to several fibres shown in figure 22. On the resin fracture surface marks can be observed indicating the crack propagation direction.

- Fatigue fracture

The photographs of cross plied carbon/epoxy fatigue specimens are shown in figures 23 and 24. The specimens have been tested at constant amplitude loading for R > 0. Fatigue failure initiation started by delamination at the edges of the specimens. Failure occurred after continued delamination.

Figure 25 shows the transition of the zone with fatigue damage to that of residual fracture.

There was a strong interface, since at numerous locations on the overload part of the fracture surface integral units of broken fibres can be observed, figure 26.

Delamination due to fatigue loading results in a different fracture surface appearance in comparison with a delamination fracture surface caused by static loading (cf. Figs. 27, 28).

In figure 27, the fatigue failure, the surface is smooth and no resin particles adhere to the carbon fibres. During fatigue loading partial debonding of the fibre matrix interface probably occurred first, after which the matrix between the fibres failed by decohesion. The laminar shear fracture surface due to static loading, figure 28,

is rather rough and interface debonding is less evident. The difference in fracture surface appearance could be caused by the strain-rate dependency of the resin properties.

5   CONCLUSIONS

1.   The Scanning Electron Microscope (SEM) appears to be an important tool in efforts to understand the nature of composite material fracture.

2.   From a study on u.d. carbon composite material fracture surfaces, it is concluded that compressive failure is connected with a relatively smooth surface, while tensile failure is usually characterized by fibre pull-out.

3.   The strength of the fibre/matrix bond is related to the measure of fibre pull-out.

4.   The direction of load applied on the composite material can be obtained from the failure marks on the fracture surfaces of individual fibres.

5.   Fatigue loading on cross plied carbon/epoxy composites caused delamination at the edges of the fatigue specimen.

6.   Delamination under fatigue loading resulted in a fracture surface appearance different from that of an interlaminar shear failure due to static loading.

6   REFERENCES

1. Parmley, P.A.   Military aircraft
Composite materials Vol. 3 Engineering applications of composites.
Academic Press New York and London, 1974.

2. Taig, I.C. Airframe applications of advanced composites
   AGARD-LS-55, 1972.

3. Rosen, B.W. and Tensile failure criteria for fibre
   Zweben, C. composite materials
   NASA CR-2057, 1972.

4. Ewins, P.P. Tensile and compressive test specimens
   for unidirectional carbon fibre reinforced
   plastics.
   RAE TR 71217, 1971.

5. Hayashi, T. and Theory and experiments of compressive
   Koyama, K. strength of unidirectionally fiber
   reinforced composite materials.
   Proc. Int. Conf. on Mechanical Behavior
   of Materials, Vol. 5, 1972.

6. Kaminski, B.E. and Strength theories of failure for anisotropic
   Lantz, R.B. materials.
   ASTM STP 460, 1969.

7. Wu, E.M. Failure criteria to fracture mode analysis
   of composite materials.
   AGARD CP 163, 1974.

8. Owen, M.J. Fatigue of carbon-fiber reinforced
   plastics.
   Composite materials Vol. 5, Fracture and
   fatigue, Academic Press New York and
   London, 1974

9. Chamis, C.C. Micromechanics strength theories.
   Composite materials Vol. 5, Fracture and
   fatige, Academic Press New York and
   London, 1974.

10. Scola, D.A.

High modulus fibers and the fiber-resin interface in resin composites.
Composite materials, Vol. 6, Interfaces in polymer matrix composites
Academic Press, New York and London, 1974

11. Auvinet, J. and Rouchon, J.

Possibilités d'utilisation du microscope électronique a balayage pour l'étude des matériaux composites a matrice organique
AGARD CP-163, 1974.

12. Fairing, D.

Examination of fracture surfaces by Scanning Electron Microscopy
J. of Comp. Mat. Vol. 1, 1967.

13. Toy, A and Engquist, R.D.

SEM Fractography of carbon fiber reinforced P13N polyimide composites.
Scanning Electron Microscopy, 1970.
Proceedings of the 3rd annual scanning electron microscope symposium, Chicago, Illinois.

14. Johnson, W, Watt, W.

Structure of high modulus carbon fibres.
Nature, Vol. 215, 1967.

15. Gunston, W.T.

Carbon fibres.
Science Journal, Febr. 1969.

16.

Fokker report No-Fok-R-1707/Part 1-XI, 1973.

17. Kendall, E.G.

Development of metal-matrix composites reinforced with high modulus graphite fibers.
Composite materials, Vol. 4, Metallic matrix composites Academic Press, New York and London, 1974.

18. 't Hart, W.G.J., Jacobs, F.A. and Nassette, J.H.

Tensile failure of unidirectional composite materials.
NLR TR 75114 U

Fibre	Treatment	Liquid phase	Contact angle (deg)
Boron	Untreated	Epon-828	27-30
Boron	5 min wash at 70°F in acetone	Epon-828	11
Boron	5 min wash at 70°F in trichloroethylene	Epon-828	14
Boron	5 min wash in boiling ethanol	Epon-828	7
Thornel 25	Untreated	H_2O ERLA-0400 ERL -2774	36 12 ± 7 32 ± 8
Thornel 25	Heated in 2 cm^3/min O_2 stream for 15 min, 500°C, followed by thermal desorption	H_2O ERLA-0400 ERL -2774	38 ± 8 $4.3 \pm 0,6$ $5.4 \pm 0,7$

Table 1 : Contact angles between several liquids and boron and carbon fibres (Ref. 10).

specimen * **	matrix	mechanical properties (MNm^{-2})		$V_f(\%)$
tensile (waisted)	DX 231/DX 137	$\sigma_{ult} = 1080$ $E_{ult} = 125300$		55
compressive (narrow)	code 64 (Fothergill and Harvey)	$\sigma_{ult} = 860$ $E_{ult} = 80520$		45
compressive (wide)	Epikote 828/Bf$_3$MEA	$\sigma_{ult} = 9070$ $E_{ult} = 119000$		69
flexural $l/t = 25$	DX 231/DX 137	$\sigma_B = 1510$ $E_B = 93880$		52
fatigue $\pm 20°$ $\pm 30°$	LY 556/HT 907	$\sigma_{ult} = 570$ $\sigma_{ult} = 360$		66 66

Table 2 : Properties of the investigated carbon/epoxy specimens.

  * specimen dimensions according to reference 16.
 ** specimens supplied by Fokker VFW and the Technical University Delft,
                                             Aeronautical Dept.

Fig. 1
and 2

16

$$\gamma_{SV} = \gamma_{SL} + \gamma_{LV} \cos \theta$$
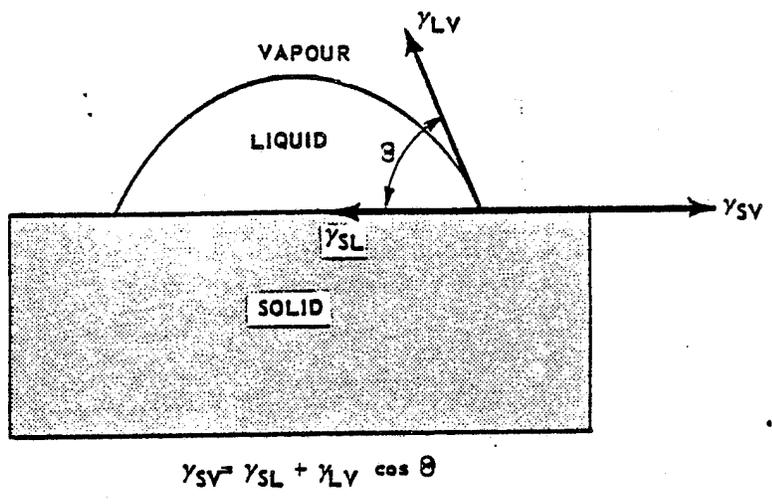
Figure 1 Equilibrium of surface energies among liquid, solid, and vapour
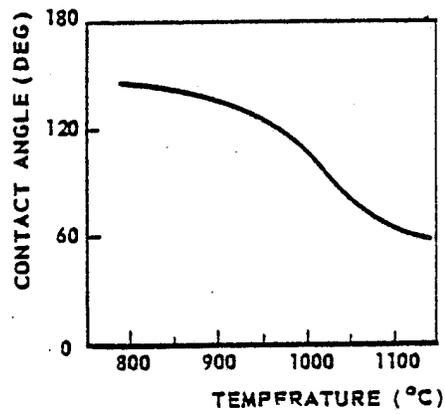
Figure 2 Contact angle of aluminium on carbon as a function of temperature (Ref.17)

Fig. 3
and 4   17

GOOD BOND   INTERMEDIATE BOND   POOR BOND

FIBRE

MATRIX

DEBONDING
NEAR THE
FIBRE ENDS
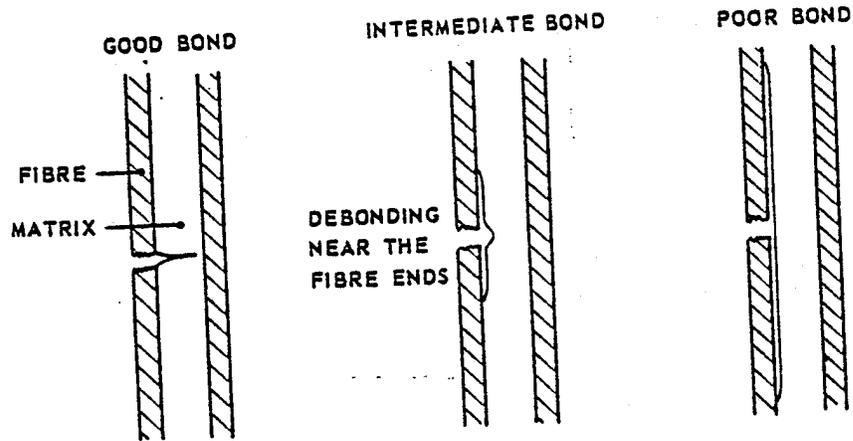
Figure 3 Influence of the interface bond on crack propagation on
a microscale

GOOD BOND   INTERMEDIATE BOND   POOR BOND

FIBRE
PULL OUT

SHEAR FAILURE
+
FIBRE PULL OUT
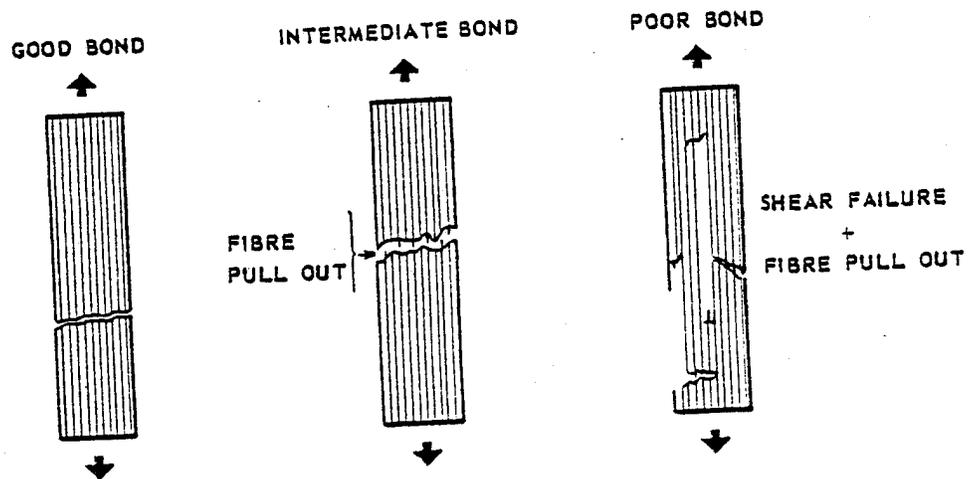
Figure 4 Longitudinal tensile failure modes in connection with
the interface bond (Ref.9)

Fig. 5
and 6

/9

APPARENT
HORIZONTAL
SHEAR STRENGTH

τ (ksi)

COMBINED SHEAR
AND
TENSION MODE | HORIZONTAL SHEAR MODE |

TENSION OR COMPRESSION
FLEXURAL FAILURE
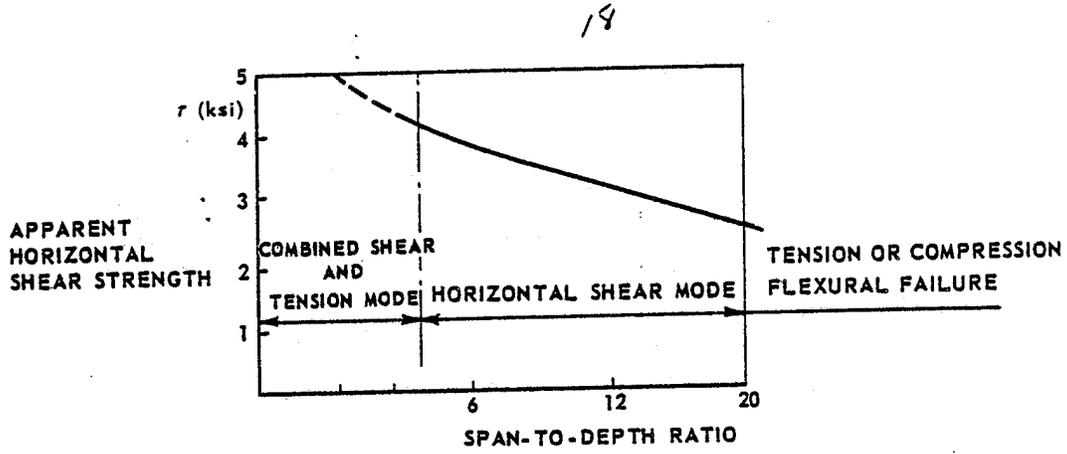
SPAN-TO-DEPTH RATIO

Figure 5   Shear strength as a function of the span-to-depth ratio
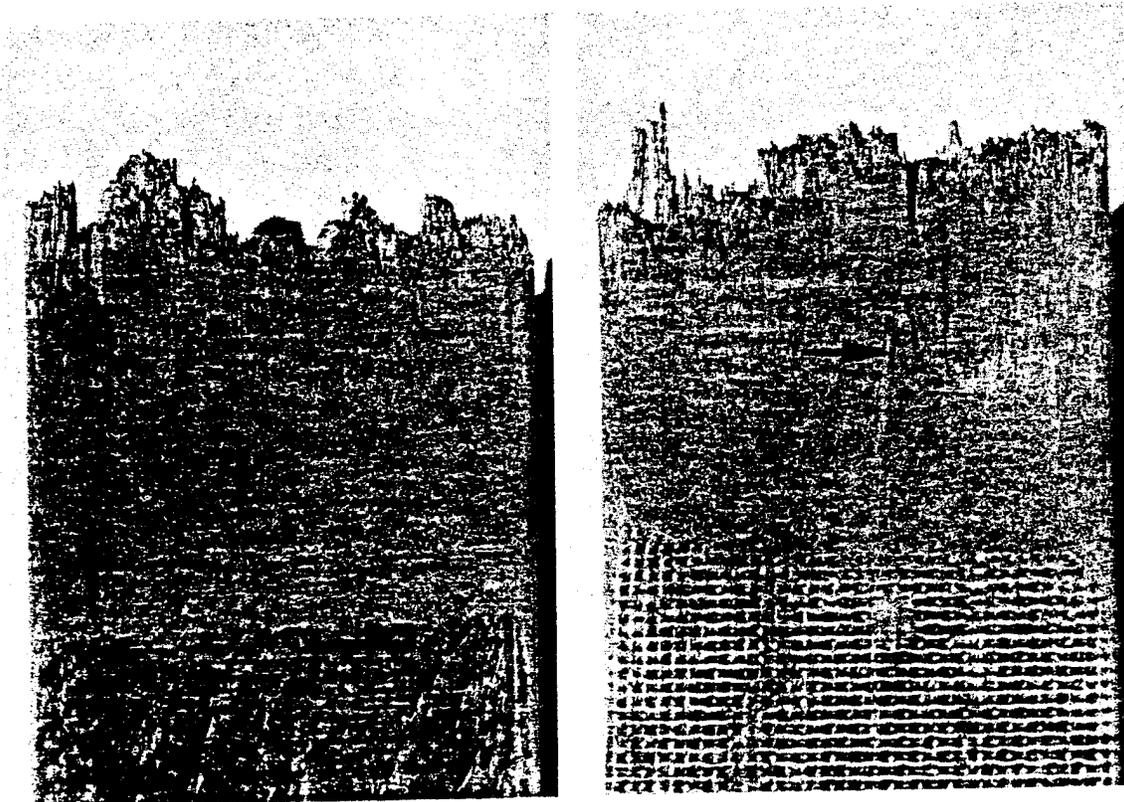
Figure 6   Fracture surfaces of a "waisted" tensile specimen

Fig. 7
and 8

19
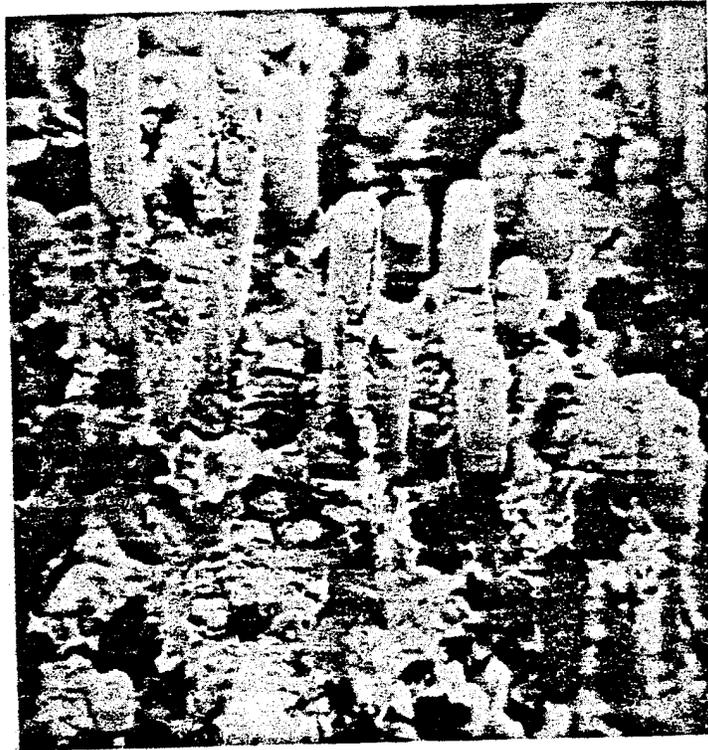
640 X

Figure 7   SEM photograph of the fracture surface shown in figure 6

4 X

4 X

Figure 8   Compressive fracture surfaces of a carbon/epoxy specimen

Fig. 9
and 10

20

3 X

FIBRE
DIRECTION

INTERLAMINAR
SHEAR FAILURE

SIDE VIEW

3 X

TOP VIEW
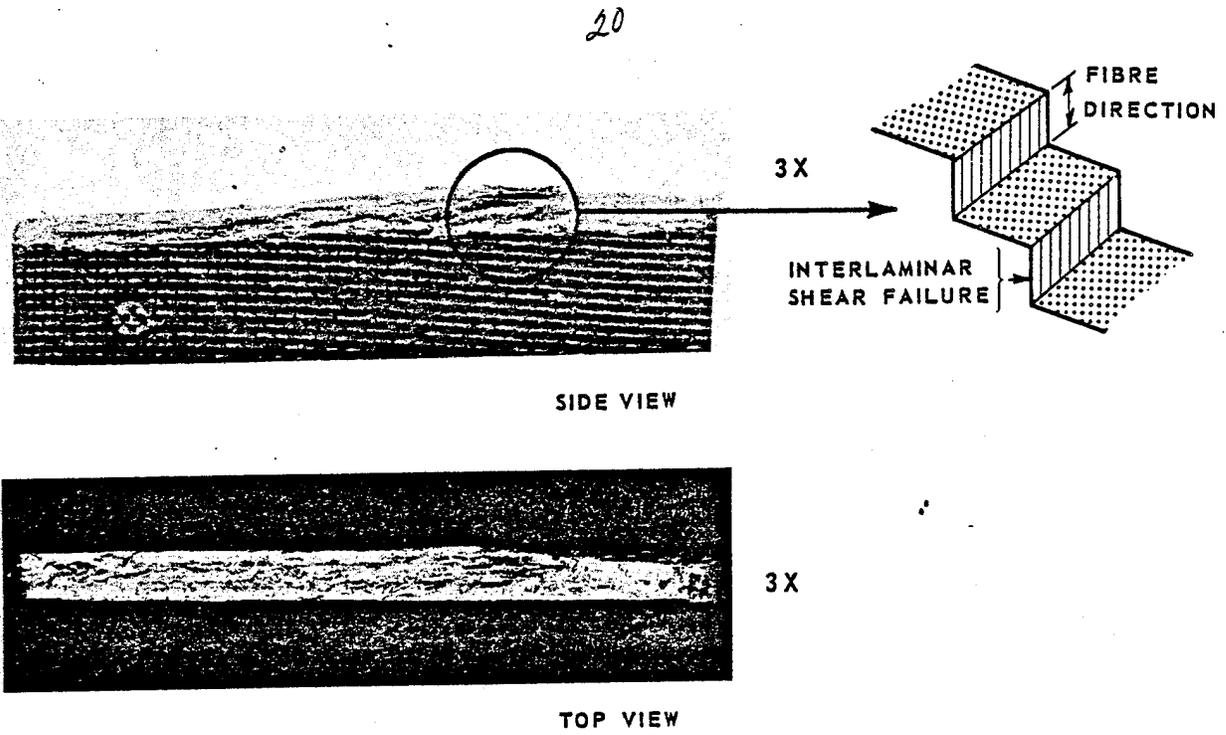
Figure 9   Compressive fracture surfaces of a carbon/epoxy specimen

630 X
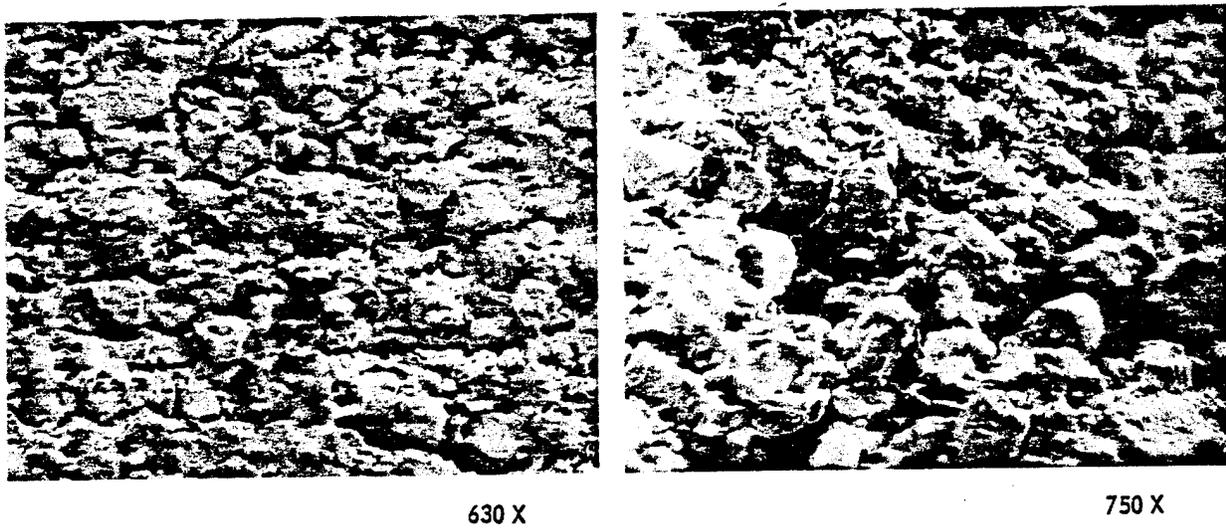
750 X

Figure 10   SEM photographs of the fracture surface of a carbon/
epoxy specimen failed under compressive loading

Fig. 11

21

SHEAR FAILURE

COMPLEX FAILURE MODE

TENSILE FAILURE
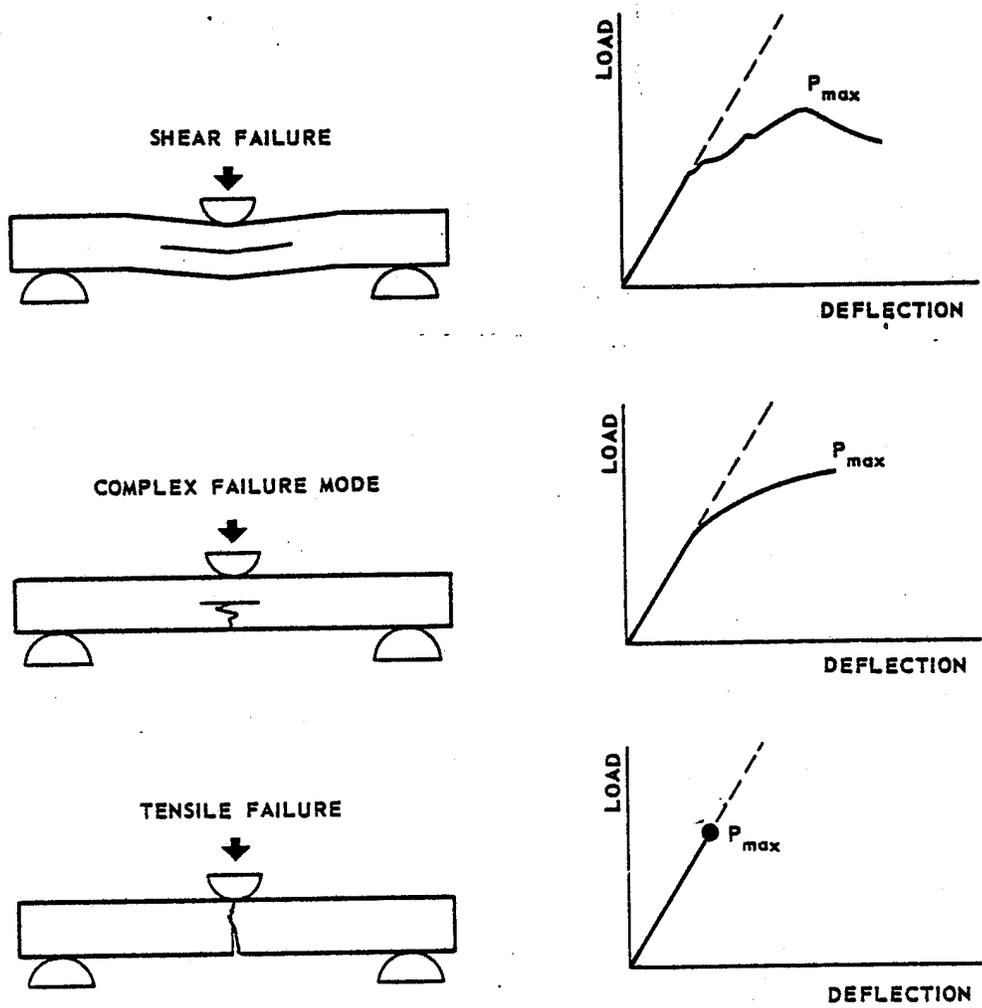
Figure 11 Types of failure in short-beam shear specimens of u.d.
composite material

Fig. 12
and 13

22

7 X   A . A   4.5 X

Figure 12 Fracture surface of a three point bend specimen

150 X

Figure 13 SEM photograph of the fracture surface shown in figure
12, at the location of the "neutral plane" (150x)

Fig. 14
and 15

23

750 X

Fig. 14
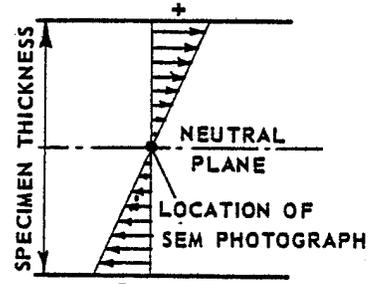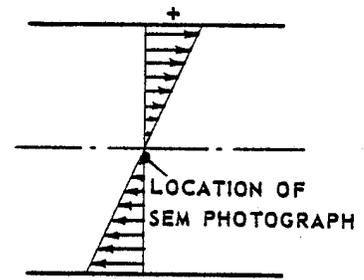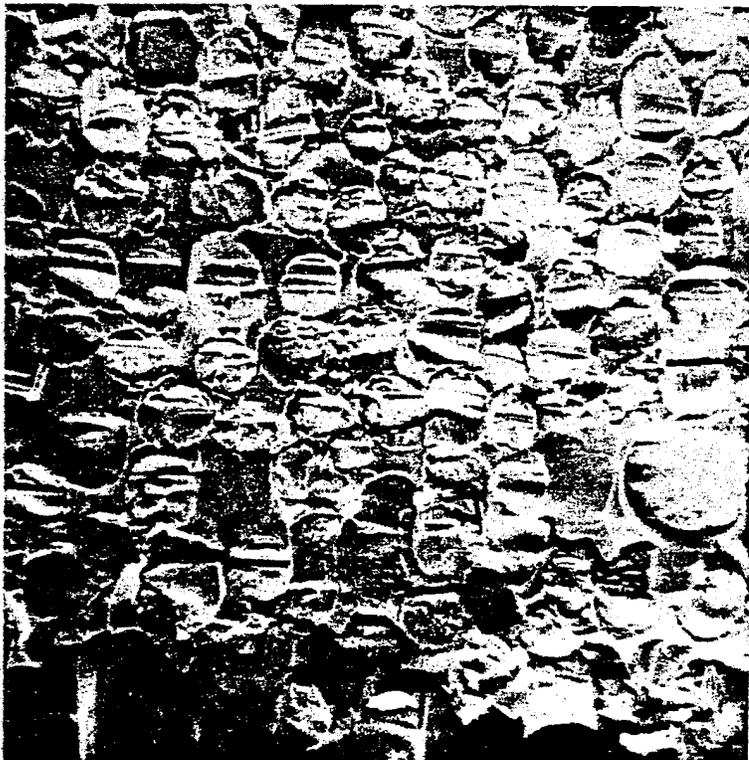
750 X

Figure 15 SEM photographs showing interlaminar shear cracks
(upper figure) and fibre buckling

Fig. 16
and 17

54

2500 X

Figure 16   SEM photograph of fibre buckling (2500x)

	FIBER MODULUS,	MATRIX MODULUS
	E_f,	E_m,
	psi	psi
————	60×10^6	0.38×10^6
– – – –	10	0.38
—·—·—	10	1.00
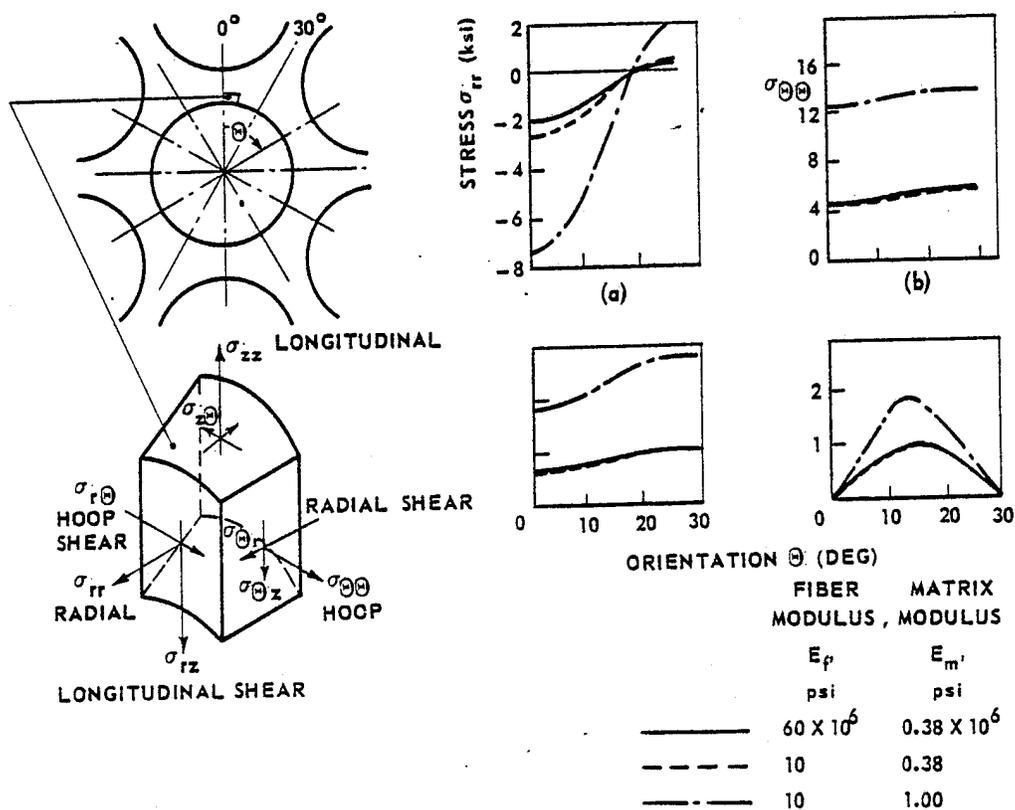
Figure 17   Residual shrinkage stresses at the interface for combinations
of fibre and resin moduli at a fibre volume ratio of 0.64 and
$\alpha_m \Delta T = 0.01$ (Ref.9)

35
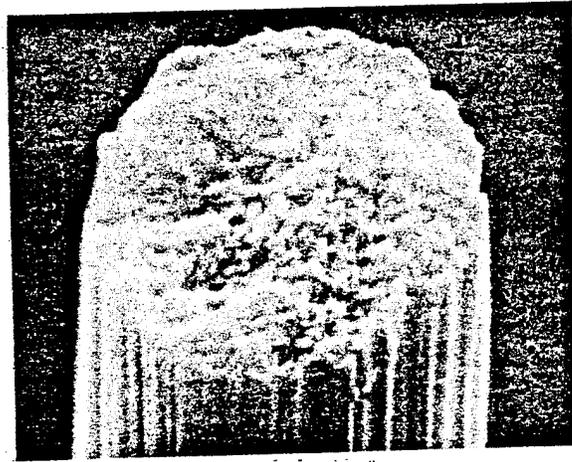
6400 X

Figure 18   Tensile fracture
                surface
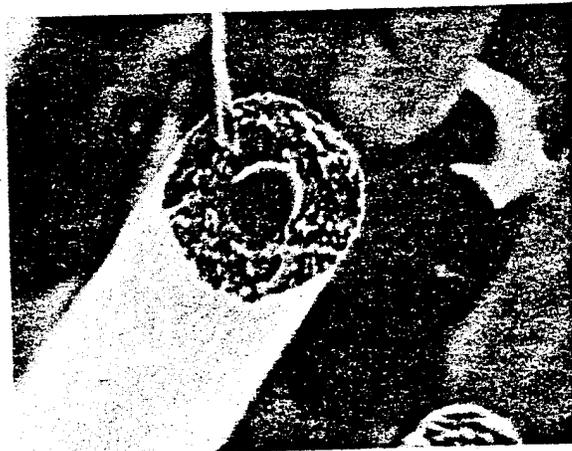
1650 X

Figure 19   A hollow carbon
                fibre

POLYACRYLONITRILE
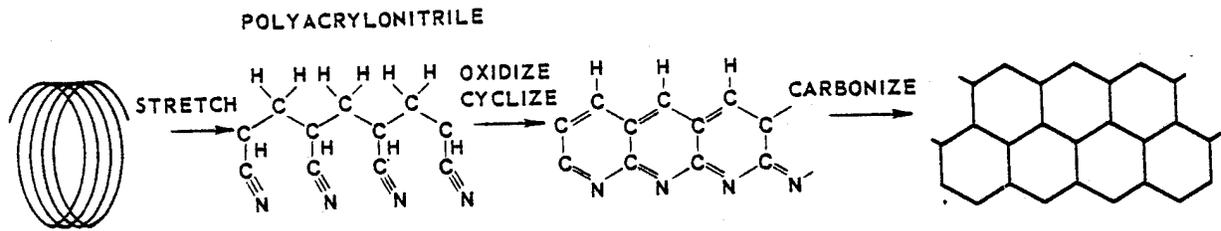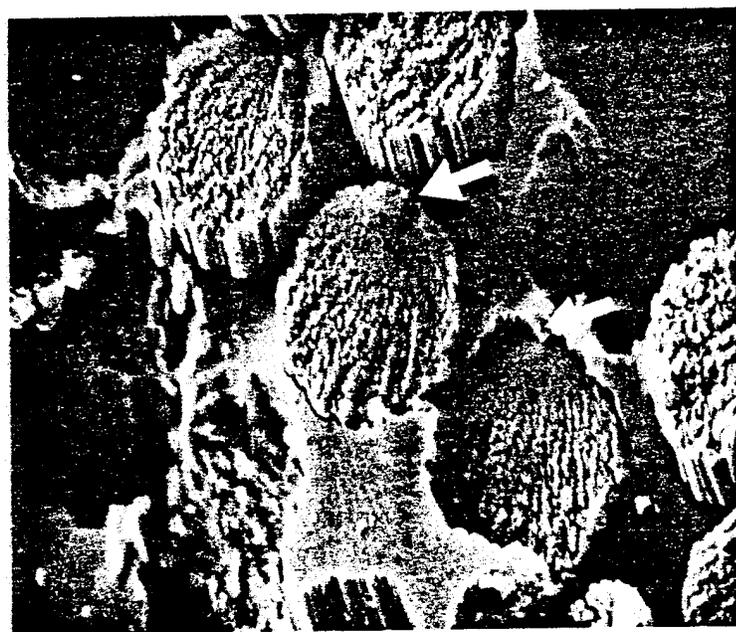

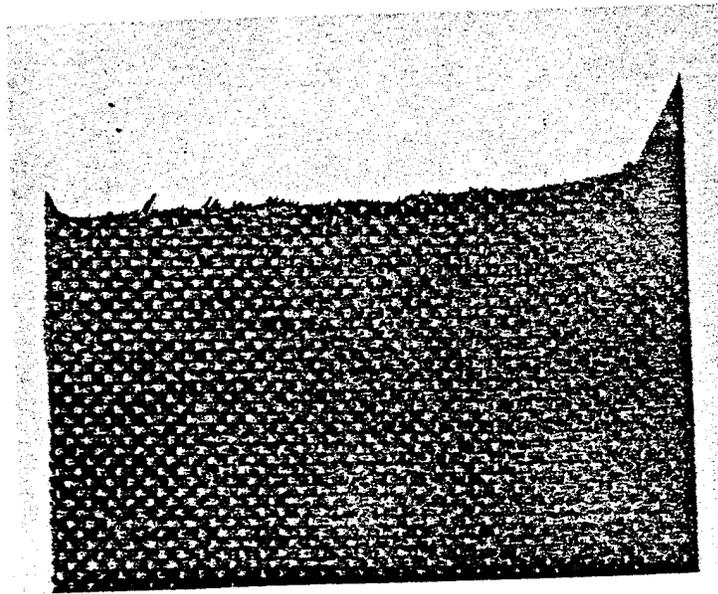Figure 20   Transition of polyacrylonitrile to carbon fibre

Fig. 21
and 22

26

SINGLE FIBRE

INDIVIDUAL FIBRILS (RIBBONLIKE)

CRYSTALLINE STRUCTURE

CROSS SECTION A - A   A

A

FIRST LATTICE PLANE
SECOND LATTICE PLANE

AMORPHOUS CARBON
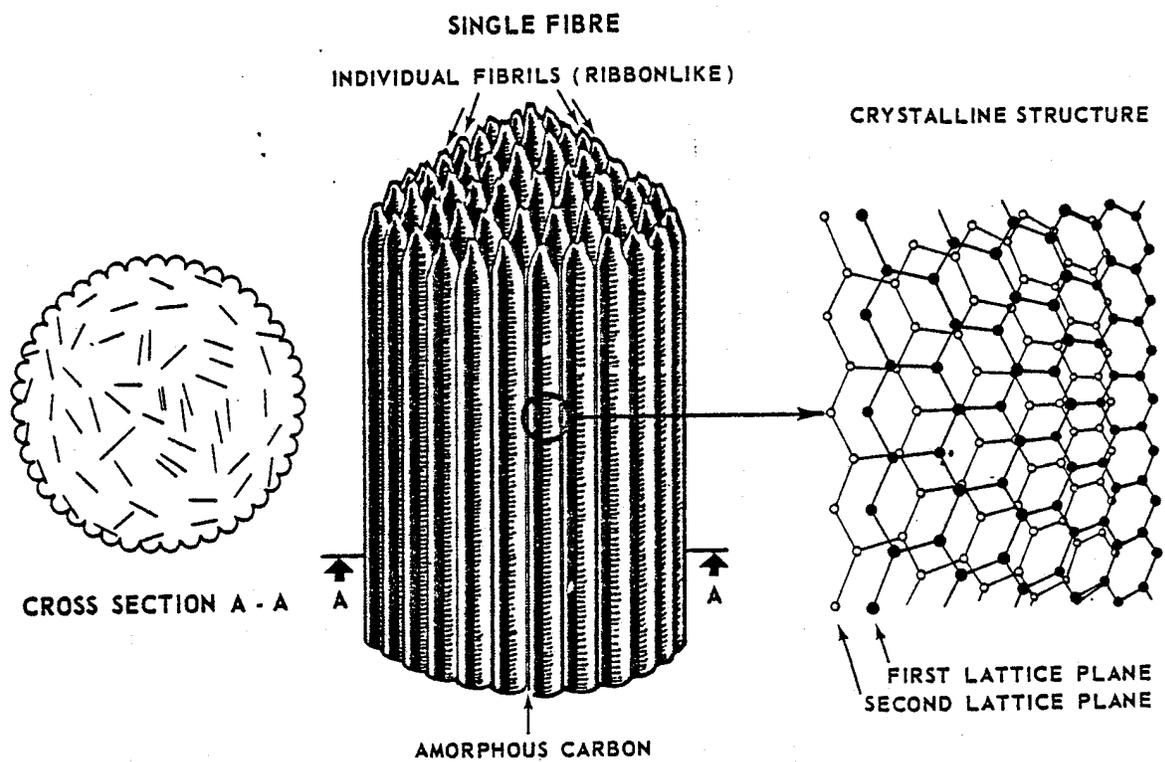
Figure 21   Building up of a carbon fibre (Ref.15)

2300 X

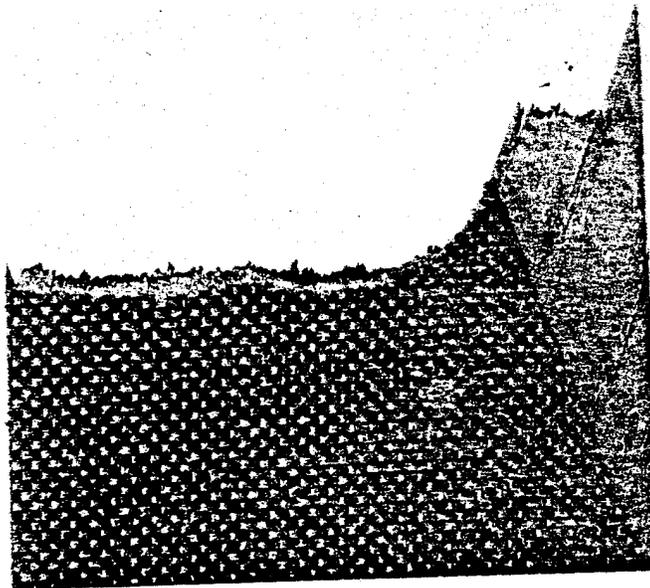Figure 22   Fracture initiation at the edge of a carbon fibre
(2300x)

Fig. 23
and 24

27

FIBRE ORIENTATION (±30°)

2X

Figure 23   Fracture surface of a carbon/epoxy specimen tested under fatigue loading

FIBRE ORIENTATION (±20°)

2X

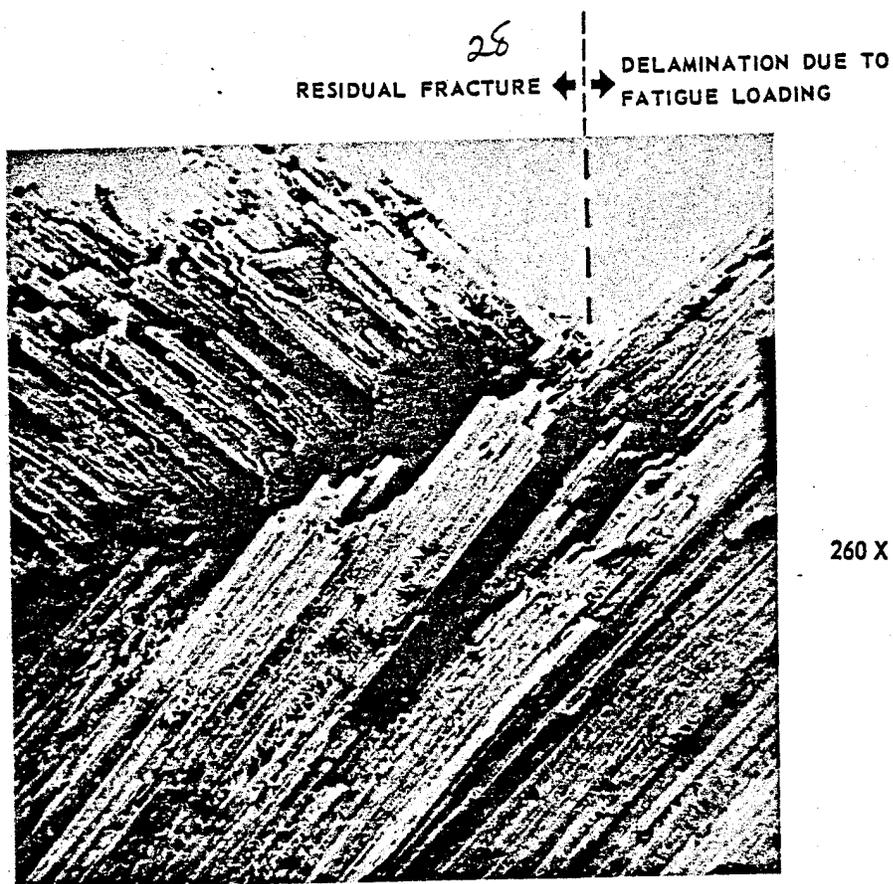Figure 24   Fracture surface of a carbon/epoxy specimen tested under fatigue loading

Fig. 25
and 26

RESIDUAL FRACTURE ← | → DELAMINATION DUE TO
FATIGUE LOADING

260 X

Figure 25 Transition of the zone with fatigue damage to that
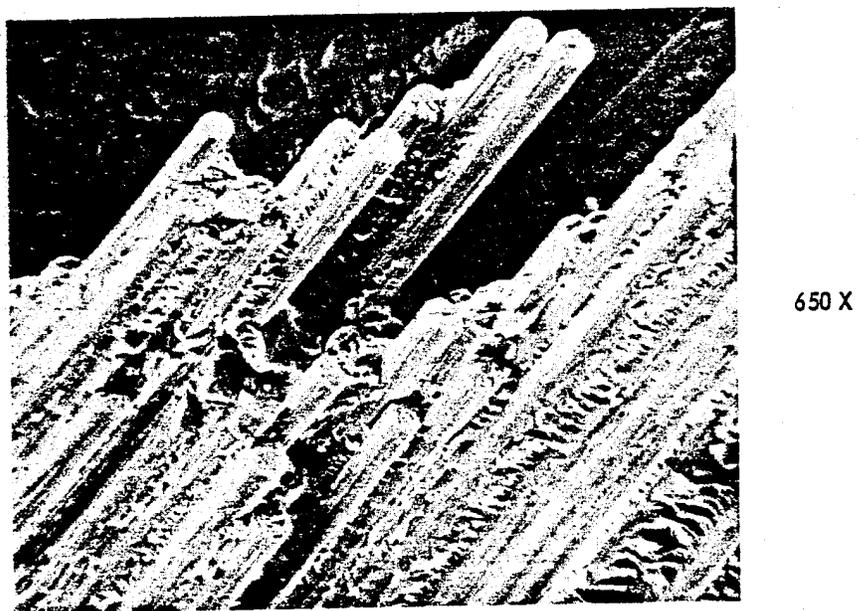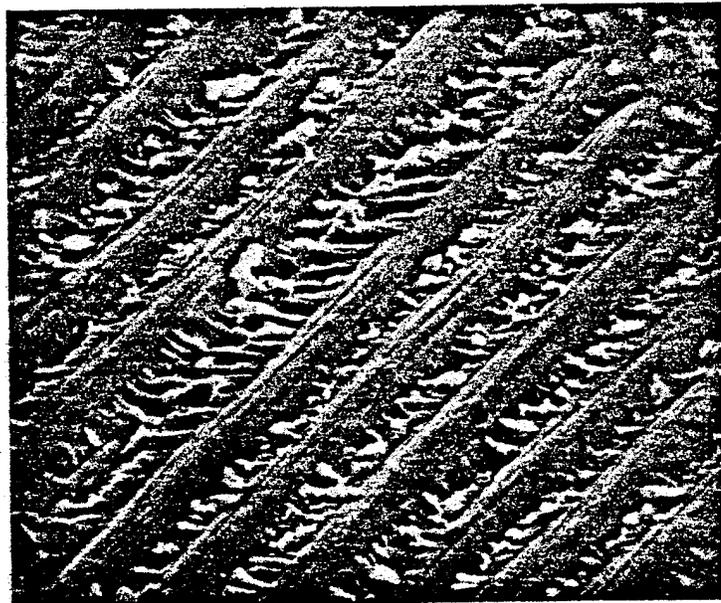of residual fracture

650 X

Figure 26 SEM photograph showing a good interface bond in the
cross plied laminate (650x)

Fig. 27
and 28

29

1240 X

Figure 27 Shear failure by fatigue delamination (1240x)

1240 X

Figure 28 Shear failure in the residual fracture surface (1240x)